

The SZ effect contribution to WMAP. A Cross-Correlation between WMAP and ROSAT.

J.M. Diego & J. Silk.

University of Oxford. Denys Wilkinson Building, 1 Keble Road, Oxford OX1 3RH, United Kingdom.

Draft version 17 June 2019

ABSTRACT

We cross-correlate WMAP and ROSAT and look for common features in both data sets. We detect a common structure which shows up clearly in the cross-power spectrum of the cross-correlation. The frequency dependence of this common structure follows the expected SZ effect frequency dependence. Assuming that this structure is due to galaxy clusters, we compute the expected cross-power spectrum for a variety of models and compare them with the expected power spectrum. We also discuss the possible sources of systematic errors of our approach.

Key words: cosmological parameters, galaxies:clusters:general

1 INTRODUCTION

The recent release of the MAP data (Bennet et al. 2003) has open a new window for studies of large scale structure based on the well known Sunyaev-Zel'dovich effect (SZ effect) (Sunyaev & Zeldovich, 1972). The SZ effect shifts the spectrum of the CMB photons to higher frequencies. This shift is redshift independent and proportional to the electron's optical depth times their *average* temperature along the line of sight. Electron temperature and optical depth are particularly high inside galaxy clusters. Thus, the SZ effect is a good tracer of clusters, even for those at high redshift. Around galaxy clusters, it is believed to be present a diffuse distribution of hot gas which can also be in the form of filaments. These filaments have not been detected due to their low contrast compared with the background (CMB or X-ray backgrounds). In X-rays (XR hereafter), the same electrons which cause the SZ effect will emit X-rays by bremsstrahlung emission. Therefore, one expects the SZ effect and the X-ray emission of galaxy clusters and filaments to be spatially correlated. Since the X-ray background and the CMB are not correlated (except at very large scales where there could be a correlation due to the integrated Sachs-Wolfe effect (Boughn et al. 1998)), a cross-correlation of an X-ray map with the CMB will enhance the signal of clusters and filaments with respect to a non cross-correlated background. This fact motivates studies like the one presented in this work.

We will be interested in studying the cross-correlation $SZ \otimes XR$ (where \otimes stands for cross-correlation). We need to define a *statistical object* to quantify that correlation. We will use the cross-power spectrum of the $SZ \otimes XR$ map as such an object. There are several advantages on using

the power spectrum over other statistical objects. First, the power spectrum contains useful information at different scales. For instance the 0 mode accounts for the correlation coefficient of the two maps. Higher modes will contain information about the fluctuations at smaller scales. One could argue that the correlation function also includes information at different scales. However, the correlation function can be affected by large scale variations (e.g Kneissl et al. 1997). On the contrary, the power spectrum at small scales will be independent of the large scale fluctuations. The modelling of the power spectrum is also easier and it can easily account for the uncertainties in the assumptions made in the model, as we will see later. The cross-power spectrum will also tell us something about the contribution of clusters and filaments to the CMB power spectrum. Previous works have claimed an excess in the CMB power spectrum (Bond et al. 2002). It is not yet clear whether or not this excess could be caused by SZ effect signal or just a non-subtracted residual (compact sources or residual noise). An independent estimation of the SZ effect power spectrum would help to clarify this point.

The reader is encouraged to refer to the recent literature for a more detailed description of the modelling of the power spectrum. In particular he/she may find interesting the general discussion made in Cooray & Sheth (2002), a SZ oriented discussion in Komatsu & Seljak (2002), Zhang & Wu (2003), or a X-ray oriented vision in Diego et al. (2003). For the MAP results the reader should refer to (Bennet et al. 2003) and for ROSAT data he/she can find all the useful information in Snowden et al. (1997). There are also several interesting works about cross-correlations between CMB and X-ray data sets (Kneissl et al. 1997, Boughn et al. 1998).

In this work the Hubble constant is given as $100 h \text{ km s}^{-1} \text{ Mpc}$.

2 CMB VS X-RAYS: MAP VS ROSAT

Before starting any description of the model, it is useful to give a brief description of the two data sets which are going to be used here (the reader should consult the original papers for a more detailed description. MAP data consists of 5 All-Sky maps at five different frequencies (23 GHz $< \nu <$ 94 GHz). At low frequencies, these maps show strong galactic emission (synchrotron and free-free). The highest frequency maps (41–94 GHz) are the cleanest in terms of galactic contaminants and will be the most interesting for our purpose. The MAP data is presented in a special format which conserves the size of the pixels and their shape (within small deviations) over the sky. This pixelisation (HEALPIX^{*}) is very appropriate for power spectrum computation. Within this pixelisation, the data is presented with a pixel size of 13.74 arcmin (Nside=256 in HEALPIX). This minimum scale will define a maximum multipole ($l = 767$) beyond which the data does not contain additional information. The units of the MAP data are temperature fluctuation with respect to the background (ΔT).

We will focus on one basic linear combination of the WMAP data, the difference $Q - W$ bands of the 1° smoothed version of the original data. This difference completely removes the main contaminant in this work, the CMB leaving a residual dominated by galactic and extragalactic foregrounds as well as filtered instrumental noise.

On the other hand, the All-Sky ROSAT All-Sky data (RASS, see Snowden et al. 1997) is presented in a set of bands ($\approx 0.1 - 2$ keV) with a pixel of 12 arcmin. Low energy bands are highly contaminated by local emission (local bubble and galaxy) while high energy bands show an important contribution from extragalactic AGN's. The optimal band for our purposes will be the band R6 ($\approx 0.9 - 1.3$ keV). This band is the best in terms of instrumental response, background contamination and cluster vs AGN emission. The pixel size is 12 arcmin and the units are cts/s/arcmin². The ROSAT maps have been *cleaned* from the most prominent point sources (all AGN's above 0.02 cts/s in the R5+R6 band have been removed). Due to the different pixel size we have repixelised ROSAT R6 band using HEALPIX and the same resolution level (Nside=256).

Although the R6 band is the *cleanest* in terms of galactic and AGN contamination, it still contains very strong emission coming from the galactic disk. In order to maximise the extragalactic signal, we should restrict our analysis to regions outside the galactic plane. In particular, we will consider only a *clean* portion of the sky above $b = 40^\circ$ and $70^\circ < \ell < 250^\circ$ which will exclude also the contribution from the north-galactic spur. This *optimal* area of the sky covers $\approx 9\%$ of the sky. As we will see later, this portion of the sky will contain an important emission coming from nearby clusters to the ROSAT R6 data.

* available at <http://www.eso.org/science/healpix>. Copyright 1997 by Eric Hivon and Krzysztof M. Gorski. All rights reserved.

As mentioned in the introduction, a CMB map will contain distortions due to the SZ effect and an X-ray map will show some structure due to the same hot and dense plasma. However, there are many differences between the two emissions which should be very well understood before modelling the power spectrum of the cross-correlation. The distortions in the CMB map are proportional to the integral of the electron density times its temperature along the line of sight. When we take the integrated signal across the area of the plasma cloud we find that (assuming $T = \text{const}$),

$$S_{\text{SZ}} = F_o \frac{TM}{D_a(z)^2} \quad (1)$$

That is, the total emission depends only on the total pressure of the plasma cloud, but not on its geometry. The constant F_o includes all the proportionality constants (baryon fraction, frequency dependence and units, $\Delta T/T$ or mJy). On the contrary, the X-ray emission by the same plasma is proportional to an integral involving the square of the electron density times the square-root of its temperature. If we now calculate the total emission from the cloud of plasma we find the surprising result that the total emission depends very much on the geometry of the cloud. This comes from the fact that the bremsstrahlung X-ray emission involves two particles and therefore the denser parts of the cloud will have a much larger emission rate than the less dense parts. Meanwhile, the SZ effect can be very well modelled if we only know the amount of gas and its temperature, the X-ray emission involves one more unknown degree of freedom, the density profile of the electron cloud for which we do not know much. Actual observations of the X-ray emission in galaxy clusters find that the observed total emission can not be reconciled with the predictions from simple analytical models. We need to include additional phenomena in the model (pre-heating, cooling flows, clumpiness) to explain this discrepancy. This suggests that pure modelling of the X-ray emission can produce predictions which are far away from the observations. In this paper we will try to overcome this problem by modelling the X-ray emission using phenomenological forms which match the observations. Thus, we will model the total X-ray emission as;

$$S_{\text{XR}} = \frac{Lx}{4\pi D_l(z)^2} = \frac{L_o T^\alpha (1+z)^\psi}{4\pi D_l(z)^2} \quad (2)$$

where Lx is the X-ray luminosity and the parameters L_o , α and ψ will be chosen to match the observed $L_x - T$ relation. In modelling the temperature in both equations (1 and 2) we will use the relation,

$$T = T_o M^\beta (1+z)^\phi \quad (3)$$

The specific values of T_o , β and ϕ will be discussed later.

3 THE CLUSTER CROSS-POWER SPECTRUM

The previous discussion relates the mm and the X-ray emission from the same plasma. However, our two data sets will include other components which could (and eventually will) show a contribution to the power spectrum. Before modelling this, it is interesting to discuss what else do we expect

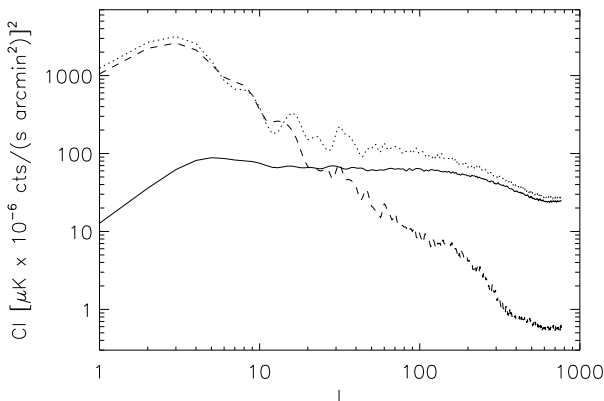


Figure 1. Power spectrum of the cross-correlated maps in three situations (this is not real data! just simulations which look like the real data. See text). Dotted line, power spectrum of a simulated MAP data (simulated CMB plus simulated SZ effect) correlated with simulated ROSAT data (simulated ROSAT noise plus simulated X-ray cluster emission). Dashed line is the power spectrum of the simulated CMB correlated with the simulated ROSAT noise. The solid line shows the power spectrum of the simulated SZ effect correlated with the simulated X-ray emission from galaxy clusters.

to contribute. We can split our data in two components, signal and residual. The signal in our case will be the emission (mm or X-ray) of galaxy clusters and filaments. The residual will include all the rest. That is, CMB, all the foregrounds, unresolved radio sources and the instrumental noise for the case of the MAP data and non-removed AGN's (see above), galactic emission, residuals left after corrections for solar flares, and/or cosmic rays plus a small contribution coming from intrinsic instrumental read-out noise in the ROSAT case.

When we cross-correlate the MAP and ROSAT maps, there will be a contribution to the power spectrum coming from these residuals. Even if the MAP and ROSAT residuals are not correlated, the power spectrum of the cross-correlated map will show *features* which are common to some (or both) of the residuals. The easiest way of thinking on this is by imaging what should we expect in a simple toy model. Let's take for instance two maps A, and B which are not correlated (correlation coefficient = 0). Model A will be an All-Sky map containing a dipole (just the dipole) and model B an All-Sky map containing pure white Gaussian noise. If we cross-correlate the maps we will find that the cross correlation coefficient (the monopole) is 0 as expected but the cross correlated map will show a strong dipole so the dipole of the cross-correlation will be different from 0. We can conclude that the power spectrum contains much more information than just the correlation coefficient.

The next interesting think we should note is that when we cross-correlate MAP with ROSAT the total power spectrum will be the sum of two power spectrum.

$$C_l^\otimes = C_{l,\xi}^\otimes + C_{l,c}^\otimes \quad (4)$$

where C_l^\otimes is the power spectrum of the cross-correlated maps, $C_{l,\xi}^\otimes$ the power spectrum of the cross-correlation of

the residuals and $C_{l,c}^\otimes$ the power spectrum due to the clusters (and filaments) cross-correlation between the mm and X-ray band. The previous equation follows from the simple assumption that the cluster and filament signal is not correlated with any of the other components. This discussion can be illustrated with a simple example. In figure 1 we consider a simple example where the CMB data contains just CMB and SZ effect and the X-ray data contains only X-ray emission from galaxy clusters and some noise. The CMB was simulated using the HEALPIX subroutine synfast. The SZ effect and cluster X-ray emission were simulated based on a catalogue of more than 2700 Abell & Zwicky galaxy clusters. The masses were computed from the richness and the distances by calibrating the magnitude of the 10th brightest member with the known distances of 700 clusters. SZ effect and X-ray fluxes were computed using equations 1 and 2. The noise of ROSAT was simulated by randomising the positions of the pixels of ROSAT. This technique has the advantage that the noise map has exactly the same pdf as the original data. From figure 1 we can see how in fact the cross-correlation of the CMB map with the ROSAT noise contains structure at large scales. At smaller scales, the cross-correlation SZ effect-X-ray clusters starts to dominate the power spectrum. The total power spectrum (dotted line) can be very well described by the sum of the cluster (solid line) plus residual (dashed line) power spectra.

For modelling the term $C_{l,c}^\otimes$, we only need to know something about the cluster distribution and their signal in each band. Basically, this term will be the contribution of two terms,

$$C_{l,c}^\otimes = C_{l,c}^\otimes(2h) + C_{l,c}^\otimes(1h) \quad (5)$$

The first term accounts for the two-halo contribution and it includes the contributions to the power spectrum due to the cluster-cluster spatial correlation. This term will be significant only at very large scales. However, as we will see later, the power spectrum at large scales will be dominated by the power spectrum of the cross-correlated residuals, $C_{l,\xi}^\otimes$. The modelling of the two-halo component is a rather complicated process involving several assumptions about the bias and its evolution. We will not consider the two-halo contribution in this work but we will discuss briefly its effect later. The main contribution at small scales will come from the single-halo contribution ($C_{l,c}^\otimes(1h)$). This is just given by,

$$C_l = \int dz \frac{dV(z)}{dz} \int dM \frac{dN(M, z)}{dM} p_l(M, z) \quad (6)$$

where $dV(z)/dz$ is the volume element, $dN(M, z)/dM$ is the cluster mass function and $p_l(M, z)$ is the power spectrum (multipole decomposition) of the $SZ \otimes XR$ cross-correlated 2D profile of a cluster with mass M at redshift z . In this work we will assume Press-Schechter for the mass function (Press & Schechter 1974) although other approaches could be easily incorporated in the previous formula.

The term $p_l(M, z)$ can be modelled as,

$$p_l(M, z) = p_o(M, z) * f(l, M, z) \quad (7)$$

where p_o is just the total signal of the $SZ \otimes XR$ cross-correlated 2D profile and $f(l, M, z)$ contains the multipole dependence which depends only on the geometry of the 2D

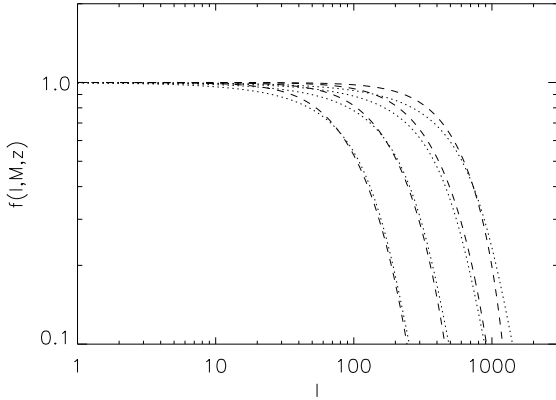


Figure 2. Multipole decomposition of the 2D cross-correlated profile for different core radii (R_c). From left to right. $R_c = 27, 13.7, 7, 3.5$ arcmin. The dashed line represents the real multipole decomposition and the dotted line is the numerical fit of equation 8.

profile. This term can be fitted numerically by the following expression,

$$f(l, M, z) = \frac{1}{2} \left(\exp(-\Sigma_{l, R_c}) + \exp(-\sqrt{\Sigma_{l, R_c}}) \right) \quad (8)$$

with,

$$\Sigma_{l, R_c} = l^2 R_c^{2/(0.97+0.68e-4/R_c)} \quad (9)$$

where the core radius, R_c , is given in rads (see figure 2). The specific shape of $f(l, M, z)$ will depend only on the geometry of the cluster. We model that geometry as a β -model with $\beta = 2/3$. Other possibilities will be discussed later. The central density is irrelevant for us since we normalise the total signal using equations 1 and 2. The only relevant parameters will be the core radius and the ratio $p = \text{virial}/\text{core radius}$ which we fix to $p = 10$ and will discuss other options later.

In terms of observable quantities, p_o can be expressed as,

$$p_o(M, z) = 4\pi |\text{Mean}|^2 \quad (10)$$

where *Mean* is the mean signal of the cluster on the sky. That is, the product of the sky-averaged mm signal (\bar{S}_{SZ}) times the X-ray signal (\bar{S}_{XR})

$$\bar{S}_{SZ}(\theta) = \frac{S_{SZ}}{4\pi} \frac{A(\theta)}{Tot(A)} \quad (11)$$

$$\bar{S}_{XR}(\theta) = \frac{S_{XR}}{4\pi} \frac{B(\theta)}{Tot(B)} \quad (12)$$

The factors $A(\theta)/Tot(A)$ and $B(\theta)/Tot(B)$ account for the profile dependence of the signal. It is important to include them because, as compared with the power spectrum in the X-rays or the SZ effect (see Diego et al. 2003), *Mean* will depend on the assumed profile. From the two previous equation it is easy to show that,

$$\text{Mean} = \frac{S_{SZ}}{4\pi} \frac{S_{XR}}{4\pi} \frac{Tot(AB)}{Tot(A)Tot(B)} \quad (13)$$

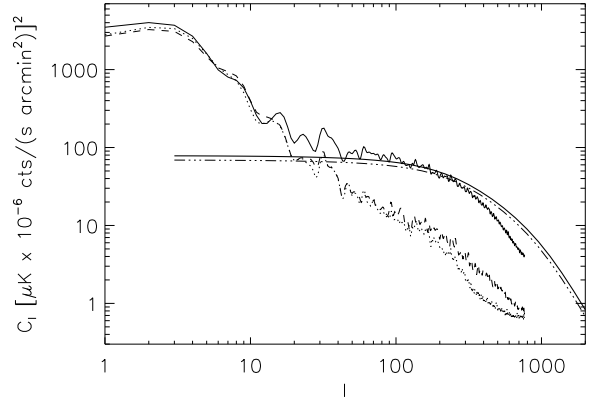


Figure 3. Thick solid line, predicted power spectrum of the cross-correlation XR-SZ for a flat Λ CDM model with $\sigma_8 = 0.8$ and $\Omega_m = 0.3$. The double-dot-dashed line is the contribution to the cross-power spectrum of the clusters below $z = 0.1$. The thin solid line is the case where we cross correlate a CMB simulation plus a SZ effect simulation (based on a catalogue of Abell clusters) with the ROSAT R6 band data. In the dashed line we rotate the simulated SZ effect 180 deg in the direction E-W. The dotted line is the power of the cross-correlation between $CMB+SZ_{Abell}$ and a random realisation of the ROSAT data.

Table 1. Reference model. All numbers are dimensionless except L_o which is given in units of $10^{42}h^{-2}\text{erg/s}$, T_o which is in keV and r_o in $h^{-1}\text{Mpc}$. This model is in perfect agreement with several cluster data sets (Diego et al. 2001, Diego et al. 2003)

Ω_m	σ_8	Γ	L_o	α	ψ	T_o	β	ϕ	r_o	p
0.3	0.8	0.2	1.12	3.2	1	9.48	0.75	1	1.3	10

where $Tot(AB)$ is the integrated 2D profile of the cross-correlated $SZ \otimes XR$ image while $Tot(A)$ and $Tot(B)$ are the integrated profiles of the SZ effect and X-ray 2D profiles respectively. Then, the only thing we need to compute the cluster $SZ \otimes XR$ cross-power spectrum is to define the scaling relations (equations 1 and 2) and give an expression for the core radius as a function of mass and redshift. For the scaling relations we will use the best fitting model found in Diego et al. (2001). The advantage of using that model is that the combinations of parameters of this model produce a good fit to several cluster data sets (mass function, temperature function, X-ray luminosity and flux functions). Later we will discuss other alternatives. For the core radius we will assume that this is given by the expression;

$$R_c = \frac{R_v}{p} = \frac{r_o M_{15}^{1/3} (1+z)}{p} h^{-1} \text{Mpc} \quad (14)$$

That is, we will assume that the core radius is a constant fraction of the virial radius. We will take this fraction (concentration parameter) as $p = 10$ and, again, we will discuss other alternatives later. We summarise our *reference* model in table 1. We will use this model for illustration purposes.

Once we have defined our model, we can compute the cross-power spectrum (equation 6). In figure 3 we show the

predicted cross-power spectrum (thick solid line) compared with a cross-correlation between a simulated $CMB + SZ_{Abell}$ map and ROSAT R6 band (thin solid line). The dashed line are the cross-correlation between a $CMB + SZ_{Abell}^{rot}$ map with ROSAT R6 band and the dotted line is a cross-correlation between the original $CMB + SZ_{Abell}$ map and a random realisation of the ROSAT R6 band with no structure. The SZ_{Abell} map was created from a Abell+Zwicky catalogue with more than 2700 clusters. SZ_{Abell}^{rot} is just a rotation (180° direction E-W) of the previous map. From the previous plot it is evident that we should expect a signature in the cross-power spectrum of $MAP \otimes ROSAT$ due to galaxy clusters. This signature will be due basically to nearby clusters like the Abell and Zwicky ones. This can be seen in the double-dot-dashed line where we compute the cross-power only up to $z = 0.1$. Most of the power is due to nearby clusters. It is also interesting to compare the previous plot with figure 1 where the ROSAT data was substituted by a simulation containing a simulation of X-ray galaxy clusters (based on the Abell+Zwicky catalogue) and the parameters of the reference model. The cross-correlation between the simulated clusters (figure 1) shows more power at smaller scales than the case when we cross-correlate the simulated $CMB + SZ_{Abell}$ with the real ROSAT R6 band (figure 3). This could be an indication that clusters are more extended in the real case (less power at smaller scales) than what was assumed in figure 1.

4 CONSTRAINTS FROM THE CROSS-POWER SPECTRUM

From the discussion in the previous sections, we have seen that we expect a significant cluster signal in the the cross-power spectrum of $MAP \otimes ROSAT$. This signal can be used to constrain the cosmological model and/or the cluster physics ($T - M$, $L_x - T$ relations, and cluster geometry). Using equation 6, we can predict the cross-power spectrum of clusters for a wide variety of cosmological models and different assumptions about the physics of the plasma. In figure 4 we show some examples of the dependence of the cluster cross-power spectrum with the cosmological parameters. The dependence with the cluster physics is shown in figure 7. The cross-power spectrum shows an important dependence with σ_8 and Ω_m and a weaker dependence with the shape parameter Γ . This plot illustrates the enormous possibilities of the cross-power spectrum as an independent cosmological discriminator. The drawback is that the cross-power is also very sensitive to the physics of the plasma (figure 7) so one must be very careful with the election of the scaling relations and the density profile in order to not introduce a bias in the resulting cosmological parameters. However, we can turn this apparent little problem into a very productive way of studying the intra-cluster physics. If the cosmological model is known with some accuracy, then one can use the cross-power spectrum as a way to constrain for instance the extension of the plasma cloud. From figure 7, we it is interesting to see how when the concentration parameter changes from 5 to 20, the cross-power changes increases a factor 50 (at $\ell \approx 500$). This is a unique dependence which can not be observed when one looks at the power spectrum of clusters in the mm or X-ray band (Diego et al. 2003). Only when

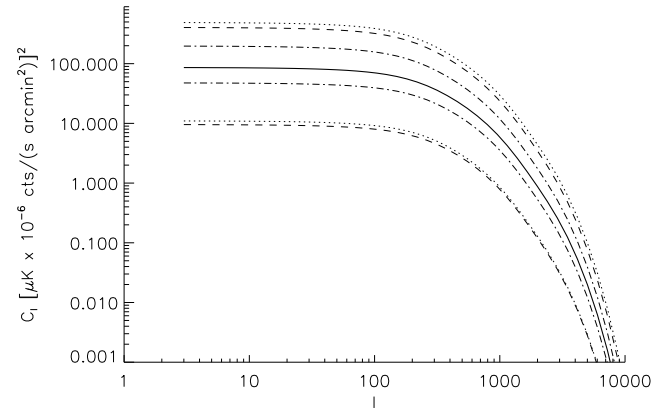


Figure 4. Dependence of the cross-power spectrum with the cosmological parameters. The solid line is the reference model of table 1. Dotted line shows the change in power when we change σ_8 0.1 units with respect to the reference model ($\sigma_8 = 0.7$ bottom, $\sigma_8 = 0.9$ top). Dashed lines show the change when we vary Ω_m 0.1 units ($\Omega_m = 0.2$ bottom and $\Omega_m = 0.4$ top). Dot dashed lines show the effect of changing Γ in 0.05 units, ($\Gamma = 0.15$ top and $\Gamma = 0.25$ bottom).

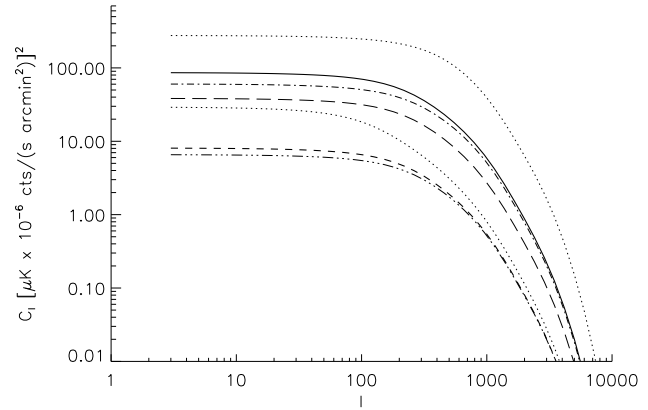


Figure 5. Dependence of the cross-power spectrum with the cluster physics. The solid line is again the reference model. The two dotted lines show the change when we take $p = 20$ (top) and $p = 5$ (bottom). If we change from $\alpha = 3.2$ to $\alpha = 2.7$, the power spectrum changes from the solid line to the triple-dot dashed line. If we change $\beta = 0.75$ to $\beta = 0.56$, the power spectrum shifts from the solid to the to the dot-dashed line. Changing L_o to $0.7L_o$ moves the solid line to the thin long-dashed line. Finally, varying T_o to $0.7T_o$ changes the solid curve to the thick sort-dashed curve.

we cross correlate these bands, we can make evident the dependence of the normalisation of the cross-power on the geometry of the cluster (see equation 13). Also interesting is to see the dependence of the cross-power with the scaling relations. In figure 7 we only illustrate the dependence with the scaling exponents α (equation 2) and β (equation 3). The dependence with ψ and ϕ will be weak since the cross-power is dominated by low redshift clusters (see figure 3).

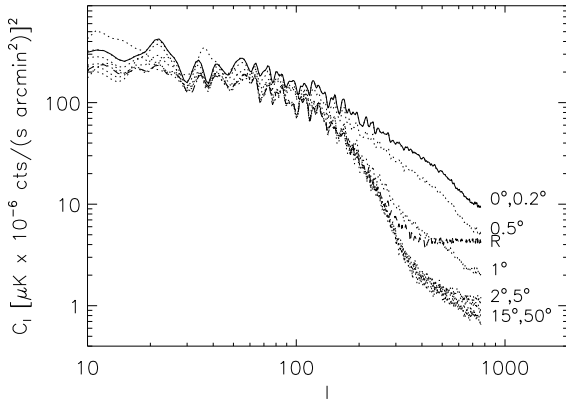


Figure 6. Cross-power spectrum of $MAP \otimes ROSAT$ (solid line). The dotted lines are the cross-power spectra when we rotate MAP between 0.2° and 50° . The dashed line (labeled R in the plot) is the cross-power of MAP cross-correlated with a random realisation of ROSAT.

It is possible to trace back the dependence of the cross-power on the scaling relations spectrum by just looking at equations 13, 1 and 2. In the case of L_o the dependence is just $C_l \propto L_o^2$. In the case of T_o the dependence is a bit more complicated since it also enters in the band correction ($B_{corr} = \exp(E_{min}(1+z)/kT) - \exp(E_{max}(1+z)/kT)$), $C_l \propto (T_o * B_{corr})^2$. The cross-power shows a weak dependence with the β exponent. A smaller exponent β will increase the temperature of the temperature of clusters with masses below $M_{15} = 10^{15} h^{-1} M_\odot$ and will decrease the temperature of clusters above that mass. The total luminosity of the clusters with $M > M_{15}$ will also increase as T^α . However, this increase is compensated by the smaller X-ray band-correction which peaks at $T \approx 1\text{keV}$ and decreases quickly for larger temperatures. The strong dependence of the cross-power with α is easier to follow since in this case the temperature do not change (and neither does the band-correction). In this case, a smaller α will produce a smaller X-ray luminosity (L_x) and consequently a smaller cross-power ($C_l \propto L_x^2$).

5 THE MAP \otimes ROSAT CROSS-POWER SPECTRUM

The cross-power spectrum of $MAP \otimes ROSAT$ is shown in figure 6. The main conclusion from this plot is that there is an excess in power with respect to the background level at scales smaller than 2 degrees ($\ell \approx 100$). The background level can be determined by rotating one of the maps. The structure due to the correlation between the maps will disappear beyond the coherence length. From figure 6, it is clear that this coherence length must be around 2 degrees since at larger angular separations the cross-power reaches the background level (bottom dotted lines). When the rotation is smaller than 0.2 degrees, we are rotating an angle which is smaller than the pixel size (13.74 arcmin). In this

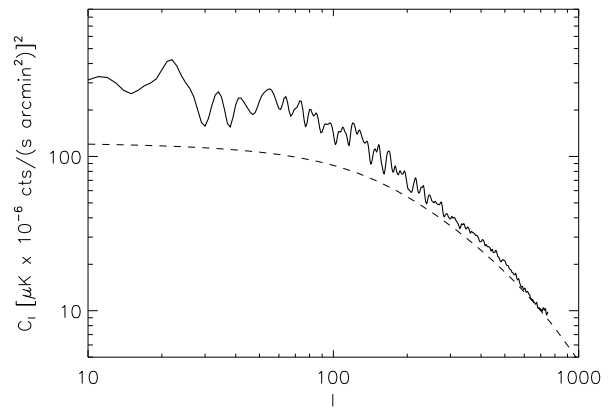


Figure 7. The cross-power spectrum (solid line) is compared with a model producing a good match to the data ($\sigma_8 = 0.8$, $\Omega_m = 0.3$), dashed line. This model is excluded by many independent cosmological tests suggesting that our estimation may suffer of systematic effects.

case the cross-power spectrum is the same as in the case with 0 rotation.

In the same plot, we also show the case when we cross-correlate MAP with a random realisation of ROSAT (dashed line). In this case, the cross-power spectrum has less power than the $MAP \otimes ROSAT$ cross-power but it has more power than the background level (bottom dotted curves). This is easy to understand since the random ROSAT realisation does not contain any structure at all (flat power spectrum) while the real ROSAT data does have that structure.

The most obvious way to reconcile all these facts; excess at $\ell > 100$, coherence length of ≈ 2 degrees, random ROSAT having more power at small than real ROSAT data (i.e. real ROSAT must have structure), is by demanding the presence of structure of scales $< 2^\circ$ which correlates between the mm and the X-ray band. A coherence length of $< 2^\circ$ could be explained by the large beam which has been used to create the smoothed maps ($FWHM \approx 1^\circ$). We have to recall that, in the cross-correlation, only the MAP data is affected by this large beam. The beam of the ROSAT data is much smaller (few arcmin). This explains why even at larger ℓ 's, the cross-power spectrum does not fall off quickly. An excess in power with the coherence length of figure 6 could be explained by correlations between a population of AGN's present in both bands. However, since the ROSAT data has been cleaned of the bright AGN's this possibility is quite unlikely. The best candidate for this excess and coherence length are then, the galaxy clusters.

The first immediate question we should address after this conclusion is what can the cross-power spectrum tell us about the population of clusters and/or their physics. When we compare the observed cross-power with our model (fixing the physical parameters of table 1) we find that the best models describing the observed power are in the correlation curve $\sigma_8 = 0.7\Omega_m^{-0.36}$. This curve contains high values of σ_{gas} which are excluded by many other methods. A lower

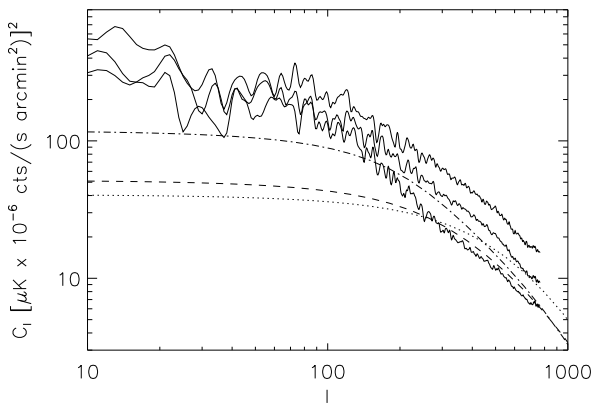


Figure 8. Solid lines: cross-power spectrum of *MAP* \otimes *ROSAT* in three different WMAP bands; from top to bottom (W-Ka), (W-Q), (W-V). The amplitude of the three bands follows the expected frequency dependence of the SZ effect. The dotted, dashed and dot-dashed lines correspond to the expected cross-power for the models A, B, and C respectively (see table ??).

Table 2. Three different models giving a reasonable fit to the observed cross-power spectrum in band (Q-W).

Model	Ω_m	σ_8	L_o	α	T_o	β	r_o	p
A	0.3	0.85	1.0	3.2	8.5	0.54	0.05	6
B	0.3	0.85	5.0	3.2	8.5	0.54	0.07	10
C	0.3	0.85	3.0	3.2	13	0.66	0.1	10

value of σ_8 could be achieved if we *fine tune* the physical parameters. For example, in figure 8 we show three models with $\sigma_8 = 0.85$ which more or less reproduce the observed power at small scales.

Also interesting is to note that the cross-power spectrum at different bands follows the expected frequency dependence of the SZ effect.

6 CONCLUSIONS

We have detected a common structure to the WMAP and ROSAT data. This structure agrees with our predictions for the case of SZE. More work in progress.

7 ACKNOWLEDGEMENTS

This research has been supported by a Marie Curie Fellowship of the European Community programme *Improving the Human Research Potential and Socio-Economic knowledge* under contract number HPMF-CT-2000-00967.

REFERENCES

Bennet et al. (more than 8 authors). 2003, submitted, astro-ph/0302

Bond J.R., et al. (more than 8 authors). 2002, ApJ submitted, astro-ph/0205386.

Boughn S. P., Crittenden R. G., Turok N., 1998, New Astronomy, vol. 3, no. 5, p. 275.

Cooray A., Sheth R., 2002, Physics Reports, Vol 372, Issue 1, 1.

Diego J.M., Martínez-González E., Sanz J.L., Cayón L., Silk J. 2001, MNRAS, 325, 1533.

Kneissl R., Egger R., Hasinger G., Soltan A.M., Trümper J., 1997, A&A, 320, 685.

Komatsu E., & Seljak U., T., 2002, MNRAS, 336, 1256.

Snowden S.L., Egger R., Freyberg M.J., McCammon D., Plucinsky P.P., Sanders W.T., Schmitt, J. H.M.M., Truemper J., Voges W. 1997, ApJ, 485, 125.

Sunyaev R.A., Zel'dovich Ya, B., 1972, A&A, 20, 189.

Zhang Y-Y., Wu X-P., 2003, ApJ, 583, 529.

This paper has been produced using the Royal Astronomical Society/Blackwell Science L^AT_EX style file.